Applied Catalysis A: General 523 (2016) 209–220

Contents lists available at ScienceDirect

Applied Catalysis A: General

journal homepage: www.elsevier.com/locate/apcata

High coverage CO adsorption and dissociation on the Co(0001) and Co(100) surfaces from DFT and thermodynamics

Congbiao Chen[a], Qiang Wang[a], Riguang Zhang[b], Bo Hou[a,*], Debao Li[a], Litao Jia[a], Baojun Wang[b]

[a] State Key Laboratory of Coal Conversion, Institute of Coal Chemistry, Chinese Academy of Science, Taiyuan 030001, Shanxi, PR China
[b] Key Laboratory of Coal Science and Technology of Ministry of Education and Shanxi Province, Taiyuan University of Technology, Taiyuan 030024, Shanxi, PR China

ARTICLE INFO

Article history:
Received 25 January 2016
Received in revised form 7 June 2016
Accepted 8 June 2016
Available online 9 June 2016

Keywords:
CO
Adsorption
Dissociation
Fischer-Tropsch synthesis
Coverage
Density functional theory

ABSTRACT

The adsorption, dissociation and desorption of CO at different coverage over two Co surfaces and the corresponding equilibrium phase diagrams under different temperatures and partial pressures have been systematically investigated; here, the results are obtained using density functional theory calculations and atomistic thermodynamics together with the periodic slab model. Our results show that the saturated adsorption on both Co(0001) and (100) surface are 7/9 ML; meanwhile, on these two surfaces, the lateral repulsive interaction has an effect on the adsorption structures and the corresponding stepwise adsorption energies of these adsorbed CO molecules, and become stronger with the increasing of CO coverage, which further leads to CO migration over Co surface; moreover, the adsorption energies decrease gradually with the increasing of CO coverage until to the saturated adsorption. According to the stepwise adsorption configurations, further calculations on CO dissociation show that only molecular adsorption CO is favored over (0001) surface; whereas on Co(100) surface, when the coverage is 1/9 ML, CO dissociation is more facile than its desorption; when the coverage is from 2/9 to 5/9 ML, only the first CO dissociation is preferred, while desorption is more favored for the left CO molecules; when the coverage is equal to or greater than 6/9 ML, CO desorption will be more favorable than its dissociation. Further, the adsorption and activation of CO under different temperatures and partial pressures from atomistic thermodynamics method well illustrate the relationship between the stable CO adsorption with the temperatures and CO partial pressure on Co(0001) and Co(100) surface, respectively. Therefore, on the basis of above results, we can obtain that the surface structures mainly affect the adsorption form of CO due to the different activity towards CO, while CO coverage will affect its adsorption energies and configurations, as well as CO dissociation on Co surfaces. The calculated stretching frequencies of CO molecule at different coverage agree with the available experimental data. This study provides a more accurate and detailed information for the process of CO adsorption and activation on Co surface.

1. Introduction

Fischer-Tropsch synthesis (FTS), that converts syngas ($CO + H_2$) to various chemical products [1–4], such as long-chain alkanes, mono-alkenes and oxygenates, has attracted great interests due to the extensive sources of syngas [5,6], in which CO adsorption is carried out on the basis of heterogeneous catalysis. Meanwhile, Co-based catalysts have been widely used in FTS due to its lower water gas shift activity, the higher selectivity and activity towards the higher carbon products, as well as the relative low cost [5,7–8]. The studies about the interaction of small molecules with catalyst surfaces is important to understand the surface structure of catalyst and the catalytic processes, moreover, it has been well recognized that CO adsorption and dissociation are the first step in FTS mechanism [9–12]. Therefore it is necessary to probe into the behavior of CO adsorption and activation on Co catalyst surfaces.

Nowadays, extensive studies have been carried out to investigate CO adsorption and activation over Co-based catalysts, and mainly focus on the ideal close-packed (0001) surface. CO adsorption on Co surface have been experimentally characterized by the thermal desorption (TPD) [13,14], work function measurements [14,15], low-energy electron diffraction (LEED) [13–17], and

* Corresponding author at: 27 South Taoyuan Road, Taiyuan, Shanxi, PR China.
E-mail address: houbo@sxicc.ac.cn (B. Hou).

http://dx.doi.org/10.1016/j.apcata.2016.06.013
0926-860X/

photoelectron spectroscopy [17,18]. It is found that CO adsorb molecularly on Co(0001) surface for temperatures up to 450 K [13,15]. At the coverage less than 1/3 of a monolayer (ML), CO adsorbs at the top site with the C—O bond normal to the surface [14–16]. At the saturation coverage, an overlayer of CO with 7/12 ML coverage has been formed. On the other hand, the theoretical studies have also been employed to investigate CO adsorption and activation over Co surface. Ge and Neurock [19] have investigated CO adsorption and activation over the flat Co(0001), as well as the stepped Co(10–12) and Co(10–24) surfaces, suggesting that CO strongly chemisorbs on these surfaces but does not show a strong dependence on the surface structure among the hexagonal close-packed (HCP) Co; the adsorption energy of CO tends to decrease as the increasing of CO coverage, in which only the coverage of 1/3, 1/4 and 1/9 ML have been considered. The studies by Cheng et al. [20] on the flat and stepped Co(0001) surfaces have suggested that both the dissociative and molecular CO adsorption are needed in FTS reaction. Ojeda et al. [9] and Gong et al. [21] have studied CO adsorption and dissociation over the $p(2 \times 2)$ and $p(3 \times 3)$ Co(0001) surface corresponding to the coverage of 1/4 and 1/9 ML, respectively. Joos et al. [22] have probed into CO adsorption and dissociation on the clean and C-covered $p(3 \times 3)$ Co(0001) surface corresponding to 1/9 ML.

As mentioned above, most of theoretical studies about CO adsorption and activation over Co surfaces are mainly carried out under its low coverage conditions from 1/9 to 1/4 ML [19–22]. Up to now, the studies about CO adsorption and activation at high coverage over Co surface are still scare, moreover, few studies have been performed to probe into the effect of coverage on CO adsorption and activation over Co surface. Moreover, the effects of temperature and CO partial pressure on CO surface coverage have not been included.

It is well known that the effects of surface structure on CO adsorption and activation usually focus on the flat and stepped surfaces that cleaved from HCP Co. However, it should be noted that Co can exist in two crystallographic structures in FTS, the hexagonal close packed (HCP) phase and the face-centered cubic (FCC) phase. It has been reported that HCP Co has higher FTS activity than FCC Co, this structure sensitivity is, however, complicated by a phase transition from HCP to FCC upon decreasing the catalyst size, varying the supports and promoters, as well as pretreating the catalysts [23–27]. Therefore, it is important to provide the useful information of CO adsorption and activation on two crystallographic Co structures. Among all Co surfaces, the (0001) and (111) surfaces are the most stable and flat surface corresponding to HCP and FCC crystallographic structures, respectively, both have the lowest surface energies of 131 and 127 meV/Å^2, respectively [23]. But there are the identical surface structures between the (0001) and (111) surfaces, which lead to the same surface properties and characteristics. Alternatively, we choose the flat (100) surface of FCC Co with the relative higher surface energies of 154 meV/Å^2, and the (100) surface is more open and exhibits the higher activity towards CO activation among all FCC Co facets. As a result, in this study, the (0001) and (100) surfaces have been chosen to consider the effect of surface structure on CO adsorption and activation.

Therefore, although the FTS mechanism is still under discussion, CO adsorption and activation are certainly attractive as an important and simple model step. In the present study, density functional theory (DFT) calculations together with atomistic thermodynamic method have been employed to investigate the adsorption, dissociation and desorption of CO molecules at diverse coverage over Co(0001) and (100) surface, as well as the corresponding equilibrium phase diagrams under different temperatures and partial pressures. It is expected that our results can provide a better understanding about the effects of coverage and surface structures on CO adsorption structures and energies over Co catalyst, the effect of temperature and CO partial pressure on CO surface coverage, and the existence form of CO over catalyst surface. Further, the mechanism of CO activation at the initial stage of FTS can be revealed.

2. Computational details

2.1. Surface model

The effects of vacuum layer, slab thickness and surface size on CO adsorption energy have been tested before the calculations of CO adsorption, dissociation and desorption at different coverage over Co surfaces. The corresponding results of CO adsorption at the hcp site on Co(0001) surface and that at the 4-fold hollow site on Co(100) surface, both are considered to be the most stable adsorption structures as presented behind, have been listed in Tables S1 and S2, respectively.

Based on above test results, a periodic $p(3 \times 3)$ supercell containing four-layers Co atoms has been employed to model Co(0001) surface, and a 12 Å vacuum layer is inserted between the periodically repeated slabs to avoid interactions. Co(0001) surface has four different adsorption sites: Top, Bridge, Hcp and Fcc, as presented in Fig. 1(a). On the other hand, for Co(100) surface, the model consists of a periodic $p(3 \times 3)$ supercell containing four-layers Co atoms, a vacuum slab of 12 Å is inserted into the direction perpendicular to the surface to separate the periodically repeated slabs, three different adsorption sites on Co(100) surface are presented in Fig. 1(b): Top, Bridge and 4-fold hollow. In all calculations, the top two layers Co atoms and all absorbed species are allowed to relax, while the bottom two layers are fixed in their bulk position.

2.2. Calculation methods

In this study, the plane-wave based density functional theory (DFT) calculations are performed with projector-augmented wave (PAW) method [28,29] that implemented in the Vienna Ab Initio Simulation Package (VASP) [30,31]. The generalized gradient approximation (GGA) proposed by Perdew-Wang (PW91) [32] is used to describe the exchange-correlation energies and potential. All calculations are spin-polarized due to the magnetic properties of cobalt with a plane wave cutoff energy of 400 eV [33], the reported structures will be converged while the energy differences are smaller than 10^{-5} eV, and the forces are less than 0.03 eV/Å. A $5 \times 5 \times 1$ k-points grid generated via the Monkhorst-Pack procedure [22,34] is used for sampling the Brillouin zone. The calculated lattice constant of bulk HCP Co is 2.49 Å, which agrees with both the experimental value of 2.51 Å [35] and other calculated values of 2.51 and 2.49 Å [9,36], respectively. Meanwhile, the calculated lattice constant of bulk FCC Co is 3.53 Å, which is in good consistent with both the experimental value of 3.54 Å [37] and other calculated values of 3.52 and 3.53 Å [38,39], respectively. Spin-polarized calculations on the isolated CO molecule, C and O atoms are carried out in a $10 \times 10 \times 10$ Å cubic unit cell with a single k-point [40]. The calculated C—O bond length of gas phase CO molecule is 1.14 Å, which also agrees with the experimental values of 1.13 Å [41]. In addition, DFT functional are well known to have the limitations for calculating CO frequency when it is bonded to transition metals, and our results also indicate that the computed stretching frequencies of CO molecule in the gas phase is 2126 cm^{-1}, which is lower by around 40 cm^{-1} than the experimental value of 2169 cm^{-1} [35].

To investigate CO dissociation on Co surface, the Climbing-image Nudged Elastic Band method (CI-NEB) [42,43] is employed, and the transition states are optimized using the dimer method [44,45]. The transition state structures will be converged when the forces for all atoms are less than 0.05 eV/Å. Vibrational frequencies

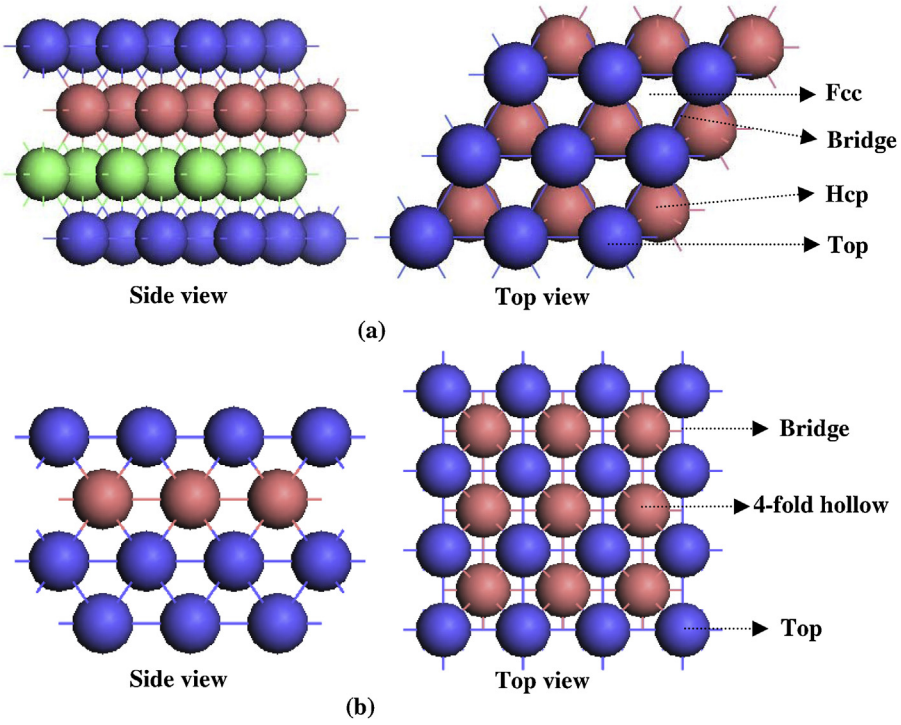

Fig. 1. The surface morphology and possible adsorption sites of (a) Co(0001) surface, (b) Co(100) surface.

for all adsorbed species were determined in single point calculations with metal atoms fixed at their positions.

2.3. Thermodynamic analysis

Given that the contributions of zero-point vibrational energy (ZPE), thermal energy and entropy to the standard molar Gibbs free energies, the thermodynamic statistical formulas derived from partition functions have been used to correct the total energy obtained directly from DFT calculations. The standard molar Gibbs free energy for gaseous and adsorbed CO species can be obtained by the following Eq. (1):

$$G^{\theta}(T,p) = E\text{total} + EZPE + U^{\theta} - TS^{\theta} + \gamma RT[1 + \ln(p_{CO}/p^{\theta})] \quad (1)$$

Where E_{total} refers to the total energy obtained directly from DFT calculations, R is the gas constant, p is the partial pressure of the gas-phase molecule, γ is 0 for surface adsorbed species and 1 for gaseous molecule; E_{ZPE} is the zero-point vibrational energy, U^{θ} and S^{θ} are the thermal energy and entropy, respectively, the detailed descriptions for the calculations methods of E_{ZPE}, U^{θ} and S^{θ} are presented in the Supplementary material. Moreover, since FTS process proceeds at the temperature range of 473–623 K under the realistic condition [46], all energies including adsorption free energy, stepwise adsorption free energy, reaction free energy barrier, reaction free energy are calculated at the temperature of 500 K.

As a convenient tool to solve problems referring to reaction conditions, atomistic thermodynamics proposed by Scheffler and Reuter [47,48] has been successfully applied to many systems [49–53]. We took CO adsorption on Co(0001) and Co(100) surfaces: Co + CO(g) → CO/Co as an example, and the change of Gibbs free energy ($\triangle G$) for this adsorption process can be described by Eq. (2):

$$\Delta G_{Co}^{ads}(T,p,n_{CO}) = G[\text{Co(slab)}/\{n_{CO}\}] - G[\text{Co(slab)}] - G_{gas}(\text{CO}) \quad (2)$$

In Eq. (2), G[Co(slab)/{n_{CO}}] is the Gibbs free energy of Co surface with n CO molecules, G[Co(slab)] is the Gibbs free energy of the pure Co surface. Compared with the great contribution of vibration to the gases, this contribution to the solid surface is negligible because of their enormous mass differences and that the vibrations involving only the metal atoms are low frequency vibrations and will mostly cancel out. Thus, we apply the total energy of the pure solid Co surface obtained directly from DFT calculation to substitute the corresponding Gibbs free energies. However, the M—C and C═O vibrations for the gaseous and adsorbed CO species need to be considered, as a result, the Gibbs free energy has been calculated for the gaseous and adsorbed CO species.

The G_{gas}(CO) term is equal to $n_{CO}\mu_{CO}(T,p)$, and the CO chemical potential can be described as Eq. (3):

$$\mu_{CO}(T,p) = E_{CO}^{total} + \widetilde{\mu}_{CO}(T,p^{\theta}) + k_B T \ln(p_{CO}/p^{\theta}) \quad (3)$$

where k_B, p_{co} and p^{θ} are the Boltzmann constant, CO partial pressure and standard atmospheric pressure, respectively. Here, we can obtained the change of Gibbs free energy during CO adsorption at different temperature T and pressure p by using Eq. (4):

$$\Delta G_{Co}^{ads}(T,p,n_{CO}) = G[\text{Co(slab)}/nCO\,] - E[\text{Co(slab)}] - nG_{CO}^{total} - n\widetilde{\mu}_{CO}(T,p^{\theta}) - nk_B T \ln(p_{CO}/p^{\theta}) \quad (4)$$

where G[Co(slab)/(nCO)] and G_{CO} are the Gibbs free energies of the corresponding systems, E[Co(slab)] is the total energies of the pure solid Co surface obtained directly from DFT calculation.

3. Results and discussion

3.1. The adsorption of the single CO molecule, C and O atoms

The adsorption free energy (E_{ads}) of these species on Co surfaces is calculated using Eq. (5):

$$E_{ads} = E_{spe/sur} - (E_{sur} + E_{spe}) + \triangle G_{ads}(\text{correction}) \quad (5)$$

where $E_{spe/sur}$ is the total energy of the adsorbed species together with the slab Co surface in the equilibrium state, E_{sur} is the total energy of the optimized bare slab surface, and E_{spe} is the total

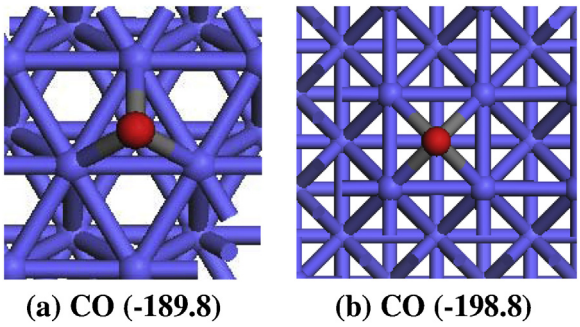

Fig. 2. The most stable adsorption configurations of the single CO molecule on Co(0001) and (100) surfaces, respectively. The Co, C and O atoms are shown in the purple, grey and red balls, respectively. The energies are in kJ mol^{-1}. (For interpretation of the references to colour in this figure legend, the reader is referred to the web version of this article.)

energy of the isolated species, $\triangle G_{ads}$(correction) refers to the change of the Gibbs free energy correction between the adsorbed systems and the gaseous species. In addition, in order to obtain the most stable adsorption site of C and O radicals, C and O adsorption energies referenced to gas-phase CO ($E_{ads,O} = E_{H2O} - E_{H2}$ and $E_{ads,C} = E_{CO} - E_O$) instead of C and O radicals, which are typically not well described by DFT [54]. Thus, the more negative values of E_{ads} denote that the adsorption is more stable than the corresponding substrate and free adsorbate. The corresponding data is presented in Figs. 2 , S1 and S2.

For the adsorption of one CO molecule, four different sites on Co(0001) surface have been examined, and the most stable adsorption configurations are presented in Fig. 2(a). CO prefers to adsorb at the hcp site via C atom with an adsorption free energy of −189.8 kJ mol^{-1}, and the C—O bond is oriented perpendicular to the surface with its length elongated from 1.14 Å in gas phase to 1.20 Å, which agrees well with the previous studies [20]. C and O atoms preferentially adsorb at the hcp site (see Fig. S1). C atom has an adsorption energy of −97.6 kJ mol^{-1} with the C—Co bond length of 1.78 Å. O atom has an adsorption energy of −14.6 kJ mol^{-1} with the O—Co bond length of 2.15 Å.

As for the adsorption of single CO molecule on the Co(100) surface, three different sites have been considered, as shown in Fig. 2(b). CO prefers to adsorb at the 4-fold hollow site with an adsorption free energy of −198.8 kJ mol^{-1}, the C—O bond is perpendicular to the surface, and the corresponding bond length is elongated to 1.22 Å from 1.14 Å in gas phase. C and O atoms prefer to adsorb at the 4-fold hollow site (see Fig. S2) with the corresponding adsorption energies of −219.2 and −52.0 kJ mol^{-1}, respectively; meanwhile, the C—Co and O—Co bond lengths are 1.88 and 1.98 Å, respectively.

3.2. CO adsorption at different coverage

To probe into the characteristics of CO adsorption over different Co surfaces, the most stable co-adsorption configurations at individual coverage on Co(0001) and (100) surfaces have been investigated, respectively, in which the numbers of CO molecules on Co surfaces are increased gradually on the basis of the most stable adsorption configuration of the single CO on Co surfaces.

The stepwise adsorption free energies of CO at different coverage are calculated using Eq. (6):

$$\Delta E_{ads} = E_{COn+1/slab} - (E_{COn/slab} + E_{CO}) + \triangle G_{ads}(\text{correction}) \quad (6)$$

where a positive ΔE_{ads} for n + 1 CO molecules indicates the saturated adsorption with n CO molecules [52,53].

As mentioned above, the hcp and 4-fold hollow sites are the most stable sites for the single CO adsorption over Co(0001) and Co(100) surfaces, respectively. Hence, in the below studies, all CO molecules are located at the most stable site in their initial configurations. Correspondingly, the most stable co-adsorption structures and the stepwise adsorption free energies of CO molecules at different coverage over Co(0001) and (100) surfaces have been displayed in Figs. 3 and 4, respectively. In addition, the stepwise adsorption energies directly obtained from DFT and all possible co-adsorption configurations have been presented in the Supplementary material (see Table S3, Figs. S3 and S4).

3.2.1. Co(0001) surface

For the coverage of 1/9–2/9 ML, CO molecules are all adsorbed at their most stable hcp sites with the C—O bond almost perpendicular to the surface, and the stepwise adsorption free energies for these CO molecules (−189.8 and −180.2 kJ mol^{-1}) are similar, suggesting that the lateral repulsive interactions between the adsorbed CO molecules are nearly negligible when the coverage is less than or equal to 2/9 ML.

For the coverage of 3/9–6/9 ML, it can be found that the corresponding adsorption free energies (−145.6, −110.7, −155.1 and −116.9 kJ mol^{-1}, respectively) are smaller than the first two CO molecules, indicating that the lateral repulsive interaction have affected the stability of CO adsorption. The adsorbed CO molecules migrate from the hcp to fcc sites, but others are very close to the bridge site, in which the first two C—Co bond become shorten and the third C—Co bond is stretched (the adsorption site in this configuration is called as like-bridge site). Moreover, with the increasing of CO coverage, more CO molecules will tend to migration to adjust the distance between the adsorbed CO molecules.

For the coverage of 7/9 ML, it can be found that CO molecules are adsorbed at the 3-fold hollow (hcp and fcc), like-bridge and top sites, suggesting that the lateral repulsive interaction obviously affects the adsorption structures and stepwise adsorption free energies of these CO molecules. And the corresponding adsorption free energies (−30.1 kJ mol^{-1}) are smaller than the first six CO molecules.

When the coverage reaches 8/9 ML on the surface, the calculated ΔE_{ads} has become a positive value of 220.4 kJ mol^{-1}, namely, it has reached the saturated adsorption over Co(0001) surface.

3.2.2. Co(100) surface

For the coverage of 1/9–2/9 ML, all CO molecules are adsorbed at their most stable 4-fold hollow sites, and the C—O bond is almost perpendicular to the surface; the adsorption free energies for the first two adsorbed CO molecules (−198.8 and −206.3 kJ mol^{-1}) are nearly same, which show that the lateral repulsive interactions between these two adsorbed CO molecules are negligible when the coverage is less than or equal to 2/9 ML.

When there are the coverage of 3/9 ML of CO molecules adsorbed on the surface, all molecules still have the most stable sites of 4-fold hollow, the corresponding adsorption free energy (−189.0 kJ mol^{-1}) is smaller than the first two CO molecules, suggesting that the lateral repulsive interaction begins to gradually affect the adsorption of CO.

For the coverage of 4/9–6/9 ML, CO molecules begin to move to the bridge site, and the corresponding adsorption free energies gradually decrease (−168.0, −170.0 and −134.1 kJ mol^{-1}). Namely, when the coverage is greater than or equal to 4/9 ML, the lateral repulsive interaction obviously affects the adsorption structures and energies of CO molecules. Thus, as the CO coverage increases, more CO molecules will migrate to the bridge site from the 4-fold hollow site.

For the coverage of 7/9 ML, due to the stronger repulsive interaction, more CO molecules begin to transfer from the initial 4-fold hollow to the bridge sites, and the corresponding adsorption

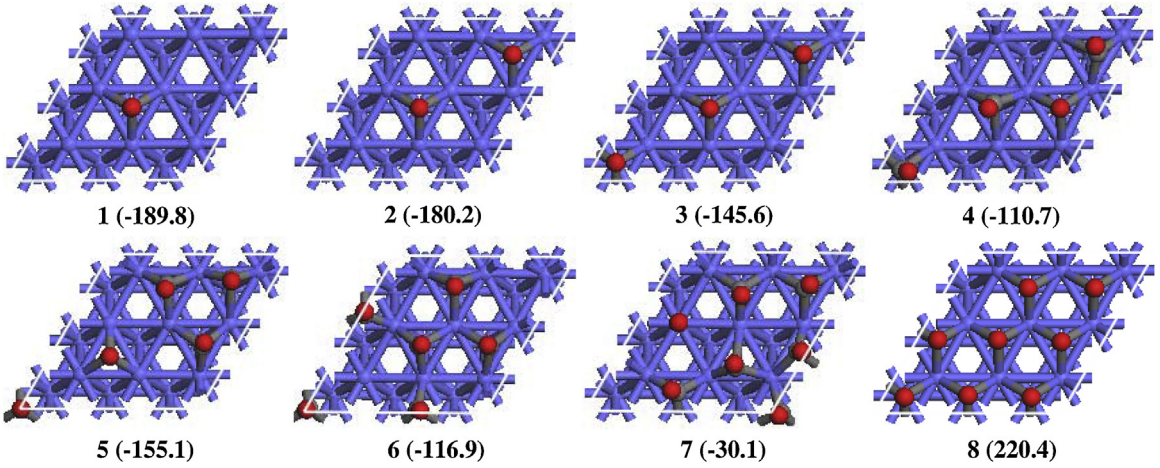

Fig. 3. The most stable configurations and the free energies for the stepwise CO adsorption on Co(0001) surface. See Fig. 2 for color coding. The energies are in kJ mol^{-1}.

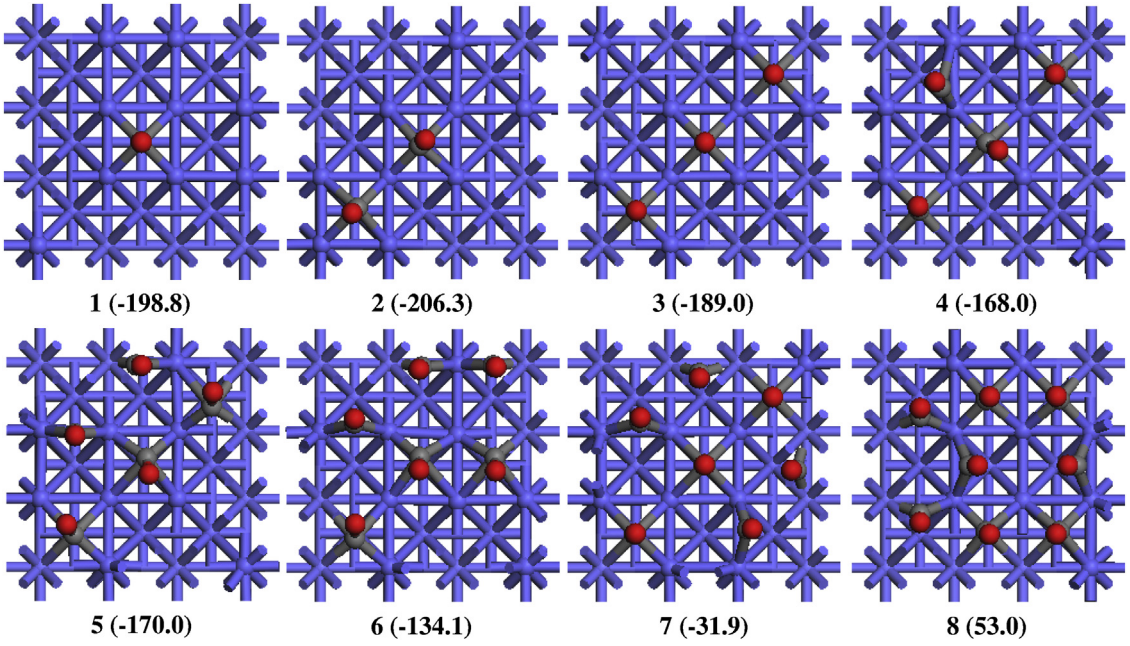

Fig. 4. The most stable configurations and the free energies for the stepwise CO adsorption on Co(100) surface. See Fig. 2 for color coding. The energies are in kJ mol^{-1}.

free energies of −31.9 kJ mol^{-1} is far smaller than the former CO molecules.

When the coverage reaches 8/9 ML on the surface, the calculated ΔE_{ads} is found to be a positive value of 53.0 kJ mol^{-1}. Thus, CO reaches the saturated adsorption with the coverage of 7/9 ML over Co(100) surface.

On the other hand, in order to re-check the most stable structures of CO adsorption at high coverage, beside the most stable adsorption site, CO adsorption at other adsorption sites are further calculated at the coverage of 6/9 and 7/9 ML over Co(0001) and Co(001) surfaces, respectively. In their initial configurations, CO molecules are adsorbed at the bridge and top sites of Co(0001) and Co(100) surface, respectively. Our results show that for CO adsorption at high coverage, the hcp sites of Co(0001) surface and the 4-fold hollow of Co(001) surface are still more stable than other sites, in their optimized configurations, CO molecules tend to migrate to the hollow sites, namely, the 3-fold and 4-fold hollow sites are more preferred for CO adsorption from low to high coverage over Co(0001) and Co(001) surfaces, respectively.

Table 1
The calculated and experimentally vibrational frequencies (υ_{CO}/cm^{-1}) of adsorbed CO from the lowest to saturated coverage over Co(0001) and (100) surfaces.

Adsorption site	Our calculated data		Experimental data	
	Co(0001)	Co(100)	Co [54]	Co(0001) [55]
hollow	1740–1829	1576–1750	1740–1830	1850
bridge	1795–1931	1879–1962	1840–2010	1900
top	2075		2030–2130	2000–2130
gas phase CO	2126		2169 [35]	

3.3. Stretching frequency of CO adsorption at different coverage

As mentioned above, the most stable adsorption configurations of CO at different coverage from 1/9 to 7/9 ML over Co(0001) and Co(100) surfaces have been obtained, we further calculated the corresponding stretching frequencies of adsorbed CO, as listed in Table 1.

On Co(0001) surface, all CO molecules are adsorbed at the hcp site with the stretching frequencies of 1740–1790 cm^{-1} for

the coverage of 1/9–3/9 ML. For the coverage of 4/9 ML, the frequency of 1852 cm^{-1} means the mixed-adsorbed CO species at the 3-fold hollow and like-bridge sites, in which the like-bridge configurations have the C—O stretching frequencies in the range of 1795–1796 cm^{-1}, CO adsorbed at the 3-fold hollow site has the stretching frequency of 1780 cm^{-1}. For the coverage of 5/9 ML, CO located at the like-bridge sites have the stretching frequencies in the range of 1813–1905 cm^{-1}, while the stretching frequency of CO at the 3-fold hollow site is 1793 cm^{-1}. For the coverage of 6/9 ML, there are two characteristic frequencies of 1940 and 1851 cm^{-1}, these signals should be attributed to the multiple-bonded CO species, which are similar to the characteristic frequency for the coverage of 4/9 ML; and the C—O stretching frequencies are 1833–1836 cm^{-1} and 1858–1861 cm^{-1} for like-bridge sites. For the coverage of 7/9 ML, three adsorption configurations coexist, and the C—O stretching frequencies are 2075 cm^{-1} for the top sites, 1870–1873 cm^{-1} for the like-bridge sites, as well as 1798–1800 cm^{-1} for the 3-fold hollow sites; besides, the stretching frequencies of 1931 and 1829 cm^{-1} are mainly attributed to the adsorption of CO at the like-bridge and 3-fold hollow sites, respectively.

On Co(100) surface, all CO molecules adsorbed at the 4-fold hollow sites have the stretching frequencies of 1607–1645 cm^{-1} for the coverage of 1/9–3/9 ML. For the coverage of 4/9–7/9 ML, the bridge configurations have the C—O stretching frequencies in the range of 1879–1962 cm^{-1}, while those at the 4-fold hollow sites are shifted to the lower stretching frequencies of 1576–1750 cm^{-1}. Moreover, with the increasing of coverage, the stretching frequencies of CO, on Co(0001) or (100) surface, are shifted to higher wave numbers, which indicates a lower activation degree of the C—O bonds at high coverage. Compared to Co(0001) surface, the C—O stretching frequencies is in the lower wave number range on (100) surface, indicating that the 4-fold hollow site have better activity than the 3-fold hollow for CO adsorption. Hence, Co(100) has better ability to activate the C—O bonds than Co(0001).

To deeply understand the adsorption properties of CO on Co surfaces, we make a direct comparison with the available experimental frequencies, as presented in Table 1. The earlier Raman spectra results [55] have reported that the vibrational frequencies of CO adsorption observed at the top sites on Co metal are 2030–2130 cm^{-1}, those at the bridge sites are 1840–2010 cm^{-1}, while those at the 3-fold hollow sites are shifted to lower wave numbers of 1740–1830 cm^{-1}. Kuipers et al. [56] have investigated CO adsorption on Co(0001) surface with RAIRS spectra, in which the vibrational frequencies observed at the top sites are 2000–2130 cm^{-1}, those at the bridge and 3-fold hollow sites are about 1900 and 1850 cm^{-1}, respectively. Although there are no available experimental data for CO adsorbed at the 4-fold hollow site, to a certain extent, our calculated results agree reasonably with the experimental frequency range on Co surfaces. Interestingly, these frequencies of 1940, 1851 and 1852 cm^{-1} agree very well with the observed characteristic frequency of 1900 and 1850 cm^{-1}, which attributed to multiple-bonded CO species on Co(0001) surface [56].

3.4. CO dissociation and desorption at different coverage

According to the most stable adsorption configurations of CO molecules that displayed in Figs. 3 and 4, the dissociation processes of these CO molecules at different coverage over Co(0001) and Co(100) surfaces have been investigated, respectively. Reaction free energy, free energy barrier and desorption free energy including the zero-point energy, thermal energy, entropies at the temperature of 500 K, and the C—O bond length in transition state for CO dissociation at different coverage over Co(0001) and Co(100) surfaces are listed in Table 2, the corresponding structures of initial states, transition states and final states for CO dissociation are presented in Figs. 5 and 6. Meanwhile, the potential energy (total energy and free energy) profile of CO dissociation at different coverage over Co(0001) and (100) surfaces (see Figs. S5 and S6 in the Supplementary Information).

For the dissociation reaction of CO on Co surface, the dissociation free energy barrier (E_a) and reaction free energy (ΔE) are calculated according to the following Eqs. (7) and (8):

$$E_a = (E_{TS} - E_{IS}) + \triangle G_a(\text{correction}) \quad (7)$$

$$\Delta E = (E_{FS} - E_{IS}) + \triangle G(\text{correction}) \quad (8)$$

Here E_{IS} and E_{FS} are the total energies of Co surface together with the adsorbed CO molecule and the dissociated C + O atoms, respectively; E_{TS} is the total energy of transition state for the corresponding dissociation reaction; $\triangle G_a$(correction) refers to the change of Gibbs free energy correction between transition states and initial states; $\triangle G$(correction) corresponds to the change of Gibbs reaction free energy correction between final states and initial states, in which the zero-point energy vibrational energy, thermal energy and entropies have been taken into consideration. Moreover, the corrected stepwise adsorption free energies are further served as the reversed stepwise desorption free energies to further carry out a comparison between the dissociation and desorption of adsorbed CO molecules over Co surface. Finally, the thermal energy and entropies, as well as the dissociation free energy barrier and reaction free energy were calculated at the temperature of 500 K and the standard pressure (p^{θ}) for gas-phase species and the adsorbed state species.

3.4.1. Co(0001) surface

For the dissociation of CO at the coverage of 1/9 ML on the Co(0001) surface, starting from the adsorbed CO, CO dissociates into C and O atoms via transition state TS1, where C and O are located at two adjacent hcp sites, as shown in Fig. 5. The dissociation free energy barrier of this elementary reaction is 235.0 kJ mol^{-1}, which is much lower than the C—O bond energy (1070.3 kJ mol^{-1}) of CO in the gas phase, and this reaction is endothermic by 94.5 kJ mol^{-1}; while the corresponding desorption free energy is 189.8 kJ mol^{-1}, suggesting that CO desorption is more favored rather than its dissociation. Previous studies have shown that the barrier of CO dissociation on Co catalyst is similar to our results in this study. Ge and Neurock [19] have reported that CO dissociation on Co(0001) surface has an activation barrier of 232.0 kJ mol^{-1}. Gong et al. [21] have obtained CO dissociation barrier of 260.0 kJ mol^{-1} on Co(0001) surface. Joos et al. [22] have also obtained the barrier and reaction energy of 221.4 and 88.5 kJ mol^{-1} for CO dissociation on Co(0001) surface. Therefore, CO dissociation on Co(0001) is expected to be an unfavorable process.

For the dissociation of CO molecules at the coverage of 2/9 ML, as shown in Fig. 5, the adsorbed two CO molecules firstly dissociate into CO + C + O via transition state TS2, subsequently, the left CO molecule dissociates into 2C + 2O via the transition state TS3, in which two C atoms and two O atoms are adsorbed at the 3-fold hollow site. The dissociation of these two CO molecules is endothermic by 123.1 and 165.9 kJ mol^{-1} with the corresponding dissociation free energy barriers of 249.5 and 260.4 kJ mol^{-1}, respectively. However, both dissociation free energy barriers of these two CO molecules are rather high compared to their corresponding desorption free energies of 180.2 and 151.7 kJ mol^{-1}, respectively, indicating that CO dissociation at this coverage is also unfavorable compared to CO desorption.

According to above results, when the coverage increases from 1/9 to 2/9 ML, the dissociation free energy barriers of adsorbed CO increase from 235.0 to 260.4 kJ mol^{-1}, the desorption free energies of these CO molecules decrease from 189.8 to 151.7 kJ mol^{-1},

Table 2
Reaction free energy ($\triangle E$), free energy barrier (E_a) and desorption free energy (E_{des}) including the zero-point energy correction, thermal energy correction, entropies at the temperature of 500 K, and the C—O bond length in transition state for CO dissociation at different coverage over Co(0001) and Co(100) surfaces.

nCO	Dissociation route	$d_{C\text{-}O}$/Å	ΔE/kJ mol^{-1}	E_a/kJ mol^{-1}	E_{des}/kJ mol^{-1}
Co(0001) surface					
1CO	1CO → 1C + 1O	1.84	94.5	235.0	189.8 (167.3)
2CO	2CO → 1CO + 1C + 1O	1.85	123.1	249.5	180.2 (164.6)
	1CO + 1C + 1O → 2C + 2O	1.83	165.9	260.4	151.7
Co(100) surface					
1CO	1CO → 1C + 1O	1.84	−46.0	131.0	198.8
2CO	2CO → 1CO + 1C + 1O	1.87	−124.2	146.9	206.3
	1CO + 1C + 1O → 2C + 2O	1.88	53.3	236.9	189.7
3CO	3CO → 2CO + 1C + 1O	1.87	−24.2	140.3	189.0
	2CO + 1C + 1O → 1CO + 2C + 2O	1.85	5.4	141.0	105.1
	1CO + 2C + 2O → 3C + 3O	1.83	16.0	213.2	112.3
4CO	4CO → 3CO + 1C + 1O	1.86	−116.0	157.8	168.0
	3CO + 1C + 1O → 2CO + 2C + 2O	1.81	−9.8	241.0	181.3
	2CO + 2C + 2O → 1CO + 3C + 3O	1.87	91.5	286.0	187.0
	1CO + 3C + 3O → 4C + 4O	3.18	236.2	246.3	151.9
5CO	5CO → 4CO + 1C + 1O	1.84	−101.5	142.4	170.0
	4CO + 1C + 1O → 3CO + 2C + 2O	1.86	88.2	331.2	148.3
6CO	6CO → 5CO + 1C + 1O	1.88	−13.0	214.6	134.1

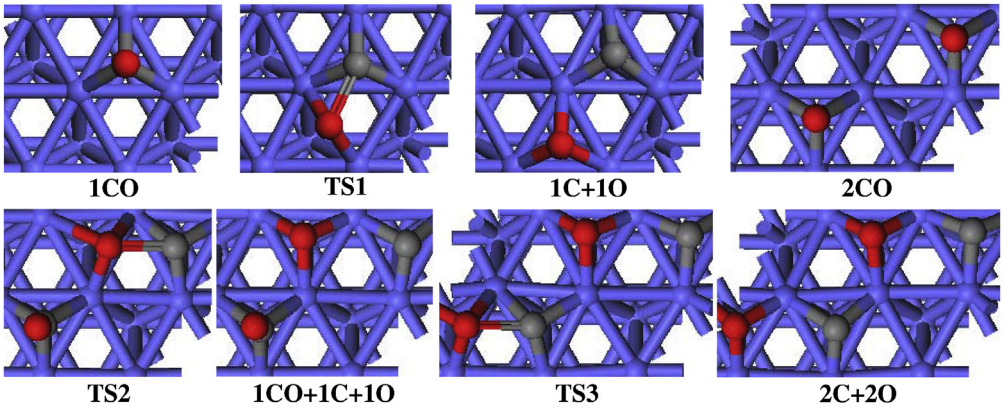

Fig. 5. Structures involved in the dissociations of 1–2CO molecules on Co(0001) surface. See Fig. 2 for color coding.

indicating that with the increasing of coverage, the dissociation barrier of adsorbed CO molecules increases, and the desorption free energy decreases. Therefore, when CO coverage is larger than or equal to 1/12 ML, the dissociation free energy barriers of adsorbed CO molecules are obviously higher than their corresponding desorption free energy, suggesting that the dissociation of adsorbed CO molecules will be unfavorable both kinetically and thermodynamically on Co(0001) surface.

3.4.2. Co(100) surface

For the dissociation of CO molecule at the coverage of 1/9 ML on Co(100) surface, CO dissociates via transition state TS1 into C and O atoms, the C and O atoms are located at two adjacent 4-fold hollow sites, as shown in Fig. 6. This elementary reaction is exothermic by 46.0 kJ mol^{-1} with a dissociation free energy barrier of 131.0 kJ mol^{-1}, which is much lower than the C—O bond energy (1070.3 kJ mol^{-1}) of CO in the gas phase, and the corresponding desorption free energy of 198.8 kJ mol^{-1}, indicating that CO dissociation is more favorable than the desorption at the coverage of 1/9 ML.

At the coverage of 2/9 ML, as shown in Fig. 6, the adsorbed two CO molecules will firstly dissociate into CO + C + O via transition state TS2, this elementary reaction is exothermic by 124.2 kJ mol^{-1}, and the dissociation free energy barrier is 146.9 kJ mol^{-1}, which is smaller than the corresponding desorption free energy of 206.3 kJ mol^{-1}. Subsequently, the left CO will dissociate through transition state TS3 to the final state, in which there are two C atoms and two O atoms adsorbed on the surface. The dissociation of the second CO molecules is endothermic by 53.3 kJ mol^{-1} with the corresponding dissociation free energy barriers of 236.9 kJ mol^{-1}, which is higher than the corresponding desorption free energies of 189.7 kJ mol^{-1}. Thus, at the coverage of 2/9 ML, there are CO molecules and dissociated C and O atoms exist on the surface.

For the coverage of 3/9 ML, these CO molecules will stepwise dissociate through the transition states TS4–6, as displayed in Fig. 6. The dissociation free energy barriers of these CO molecules are 140.3, 141.0 and 213.2 kJ mol^{-1}, respectively, and the stepwise reaction free energies are −24.2, 5.4 and 16.0 kJ mol^{-1}, respectively. While the corresponding desorption free energies of these CO molecules are 189.0, 105.1 and 112.3 kJ mol^{-1}, respectively, suggesting that at the coverage of 3/9 ML, only one CO dissociation is preferred, thus, there will be C and O atoms together with two CO molecule existed on the surface.

For CO molecules at the coverage of 4/9 ML, they dissociate successively into 4C + 4O atoms via the transition states TS7–10 with the dissociation free energy barriers of 157.8, 241.0, 286.0 and 246.3 kJ mol^{-1}, respectively, and the corresponding reaction free energies of these elementary steps are −116.0, −9.8, 91.5 and 236.2 kJ mol^{-1}, respectively. Compared to the desorption free energies of these CO molecules(168.0, 181.3, 187.0 and 151.9 kJ mol^{-1}, respectively), we can see that at the coverage of 4/9 ML, only one CO dissociation is preferred, thus, there will be C and O atoms together with three CO molecules existed on the surface.

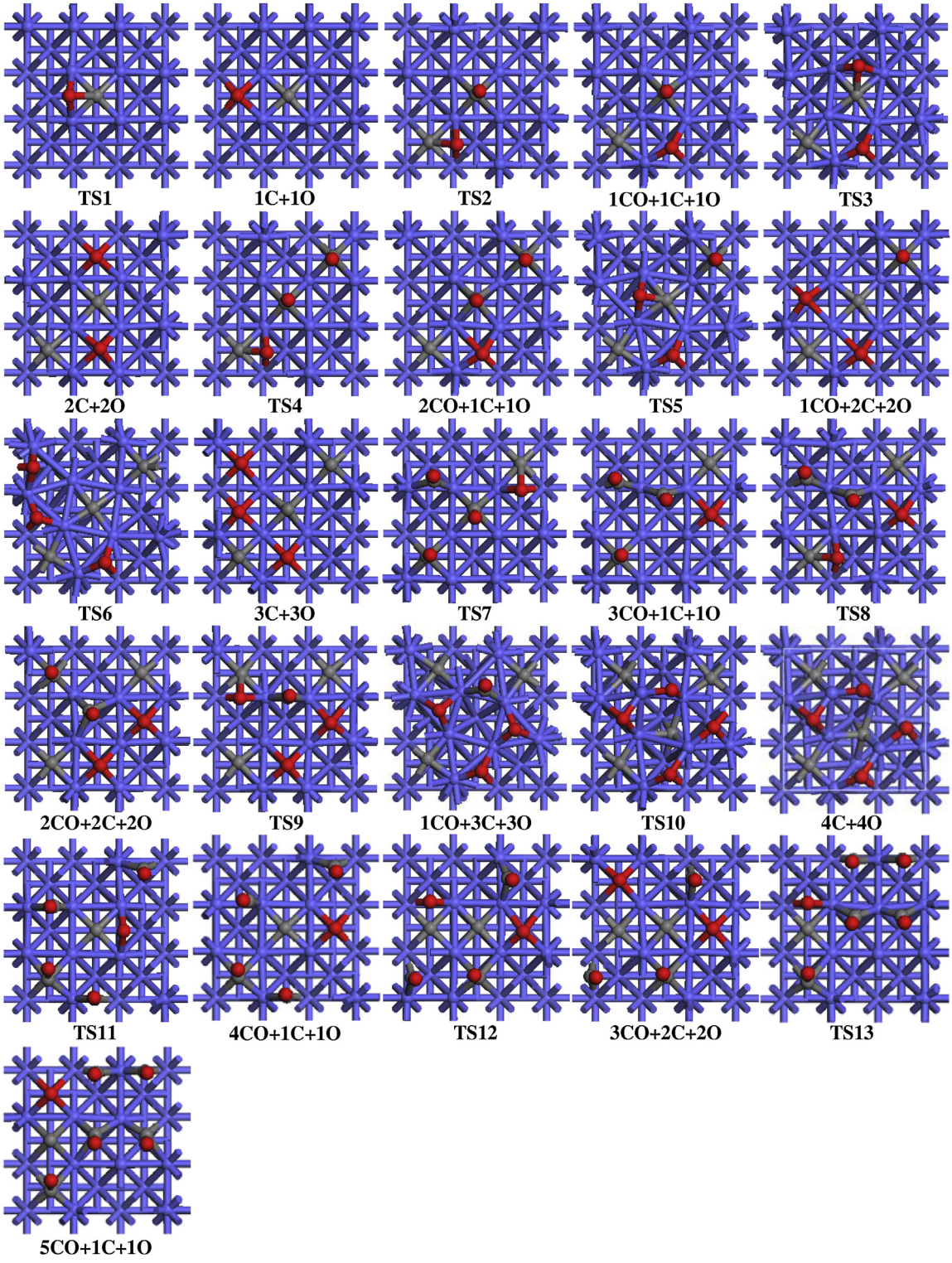

Fig. 6. Structures involved in the dissociations of 1–6 CO molecules on Co(100) surface. See Fig. 2 for color coding.

At the coverage of 5/9 ML, it is found that the first CO dissociation through the transition state TS11 has a free energy barrier of 142.4 kJ mol^{-1}, and the reaction is exothermic by 101.5 kJ mol^{-1}; while the second CO dissociates through the transition state TS12 with a free energy barrier of 331.2 kJ mol^{-1}, and the reaction is endothermic by 88.2 kJ mol^{-1}. Meanwhile, the desorption free energies of these two CO molecules are 170.0 and 148.3 kJ mol^{-1}, respectively, suggesting that at the coverage of 5/9 ML, it is also only one CO dissociation is preferred, and there will be C and O atoms together with four CO molecules on the surface.

Further, the dissociation of the first CO at the coverage of 6/9 ML is also investigated, and the calculated results show that the dissociation free energy barrier is 214.6 kJ mol^{-1}, and the reaction free energy is −13.0 kJ mol^{-1}. However, the corresponding desorption free energy is 134.1 kJ mol^{-1}, suggesting that at the coverage

greater than or equal to 6/9 ML, the dissociation of CO will be unfavorable compared to the corresponding CO desorption.

Generally, when the coverage increases from 1/9 to 6/9 ML, the dissociation free energy barriers of adsorbed CO increase from 131.0 to 331.2 kJ mol^{-1}, and the desorption free energies of these CO decrease from 206.3 to 105.1 kJ mol^{-1}, indicating that with the increasing of coverage, the dissociation barrier of adsorbed CO molecules increases, and the desorption free energy decreases, as a result, the dissociation becomes more difficult, and the desorption become easier. Moreover, with the increasing of the dissociation numbers of CO molecules on metal surface, the left free sites on surface decrease, namely, the larger the coverage of CO is, the less the left free site is, which means that CO prefer to desorb from the surface than dissociate on the surface at high coverage. Therefore, when the coverage is 1/9 ML, CO dissociation is more favorable than its desorption; when the coverage ranges from 2/9 to 5/9 ML, only the first CO dissociation is preferred, while desorption is more favored for the left CO molecules; however, the coverage is greater than or equal to 6/9 ML, CO desorption will be more favorable than its dissociation.

3.5. Microkinetic model

FTS process proceeds at the temperature range of 473–623 K [46], in order to further obtain the in-depth analysis of CO dissociation and desorption on Co(0001) and (100) surfaces under the realistic FTS conditions, we compared CO dissociation and desorption rate constants at different coverage at the temperature of 500 and 600 K respectively and further calculated CO dissociation rate using the kinetic model at the temperature of 500 K (see Tables 3 and 4). The corresponding descriptions of rate constants and kinetic model are presented in the Supplementary material.

On Co(0001) surface, at the coverage of 1/9 ML, the dissociation rate constants is far less than the desorption rate constant at 500 and 600 K, respectively; when the coverage increases to 2/9 ML, the dissociation rate constant decreases, the desorption rate constant increases comparing to the coverage of 1/9 ML, moreover, the desorption rate constants of adsorbed CO molecules are obviously higher than their corresponding dissociation rate constants, suggesting that CO prefer to desorb from the Co(0001) rather than its dissociation, these results are in agreement with that obtained by the stepwise desorption free energy.

On Co(100) surface, at the coverage of 1/9 ML, the dissociation rate constants is far greater than the desorption rate constants at 500 and 600 K, respectively, indicating that CO dissociation is more favorable than its desorption. When the coverage increases from 2/9 ML to 3/9 ML, as shown in Table 3, the dissociation of the first CO molecule remains the larger rate constant compared to that of the left CO molecules, which show that there will be C and O atoms together with two CO molecule existed on the surface. But, when the coverage reaches to 4/9 and 5/9 ML, only the dissociation and desorption of the first CO molecule will compete due to the closed rate constants compared to those at the coverage from 1/9 to 3/9 ML, and the left CO molecules will desorption. At the coverage of 6/9 ML, the desorption rate constants are much larger than the dissociation rate constants, indicating that CO begin to desorb exclusively compared to the dissociation on Co(100) surface. Thus, on Co(100) surface, there is only the dissociative adsorption of CO at the coverage of 1/9 ML, and only molecular adsorption CO is possible at the large coverage of 6/9 ML, the co-existence of the molecular and dissociative adsorption CO becomes possible at the medium coverage from 2/9 to 5/9 ML. In addition, our results show that the rate constants of both CO dissociation and desorption increase with the increasing of the temperature, namely, the high temperature can promote the dissociation and desorption of CO over Co(0001) and (100) surfaces.

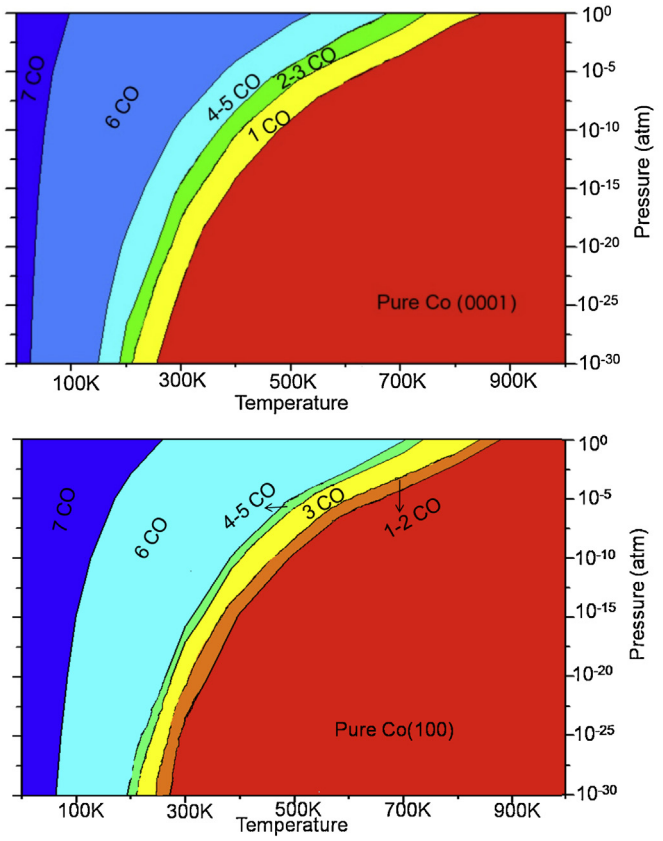

Fig. 7. Phase diagram of stable CO coverage on Co(0001) and Co(100) surfaces.

Moreover, seen from Table 4, at the coverage of 1/9 and 2/9 ML on Co(0001) surface, the negative reaction rates suggest the recombination rate of C and O is faster than the forward dissociation reaction. Thus, it is concluded that CO adsorbs molecularly on Co(0001) surface.On the other hand, on Co(100) surface, CO could dissociate fast into C andO at the coverage of 1/9 ML, and the corresponding reaction rate is 0.02 s^{-1} site^{-1}, indicating that the Co(100) has better ability for CO dissociation at the lowest coverage. At the coverage of 2/9 ML, the dissociation of the first CO molecule is obviously more facile than the second. Moreover, at the coverage between 3/9 and 5/9 ML, as shown in Table 4, with the decreasing of the free sites on the surface, CO molecule dissociation rate slowly decreases and even become negative, which suggest the recombination of C and O become favorable than the forward dissociation reaction. These results suggest CO dissociation become more difficult with the decreasing of free site at each of coverage. Further, the CO dissociation rates decrease generally as the coverage increases. Noting the dissociation rate of the first CO molecule at the coverage of 5/9 ML is abnormally close to that of the first CO molecule at 3/9 ML, which attributes to the open environment around in TS11.

3.6. CO coverage on temperature and pressure

On the basis of above discussed CO adsorption, desorption, dissociations energies and CO chemical potentials under different conditions, we plotted the equilibrium phase diagram of stable CO coverage as the functions of temperature and CO partial pressure, as shown in Fig. 7.

On Co(0001) surface, there are six regions and each region shows the possibility of getting stable CO coverage within the range of temperature or partial pressure. The first region shows the coverage of 7/9 ML (n_{CO} = 7), which is only stable at very low temperature (<30 K). The second region shows the coverage of 6/9 ML (n_{CO} = 6),

Table 3
The rate constants of the dissociation (k_{dis}) and desorption (k_{des}) of CO with different coverage at different temperature on Co(0001) and Co (100) surfaces.

nCO	Dissociation route	500 K		600 K	
		k_{dis}	k_{des}	k_{dis}	k_{des}
Co(0001) surface					
1CO	1CO → 1C + 1O	2.93×10^{-12}	1.54×10^{-7}	4.34×10^{-8}	3.74×10^{-4}
2CO	2CO → 1CO + 1C + 1O	8.94×10^{-14}	1.55×10^{-6}	2.37×10^{-9}	2.56×10^{-3}
	1CO + 1C + 1O → 2C + 2O	6.50×10^{-15}	1.48×10^{-3}	2.67×10^{-10}	0.78
Co(100) surface					
1CO	1CO → 1C + 1O	0.21	1.77×10^{-8}	49.00	6.15×10^{-5}
2CO	2CO → 1CO + 1C + 1O	4.68×10^{-3}	2.92×10^{-9}	2.03	1.37×10^{-5}
	1CO + 1C + 1O → 2C + 2O	1.85×10^{-12}	1.58×10^{-7}	2.97×10^{-8}	3.81×10^{-4}
3CO	3CO → 2CO + 1C + 1O	0.02	1.87×10^{-7}	7.62	4.39×10^{-4}
	2CO + 1C + 1O → 1CO + 2C + 2O	0.02	1.09×10^{2}	6.63	8.84×10^{2}
	1CO + 2C + 2O → 3C + 3O	5.55×10^{-10}	19.30	3.43×10^{-6}	2.09×10^{3}
4CO	4CO → 3CO + 1C + 1O	3.40×10^{-4}	2.92×10^{-5}	0.23	0.03
	3CO + 1C + 1O → 2CO + 2C + 2O	6.91×10^{-13}	1.19×10^{-6}	1.30×10^{-8}	2.05×10^{-3}
	2CO + 2C + 2O → 1CO + 3C + 3O	1.38×10^{-17}	3.03×10^{-7}	1.58×10^{-12}	6.55×10^{-4}
	1CO + 3C + 3O → 4C + 4O	1.93×10^{-13}	1.41×10^{-3}	4.50×10^{-9}	0.75
5CO	5CO → 4CO + 1C + 1O	1.38×10^{-2}	1.81×10^{-5}	5.00	1.98×10^{-2}
	4CO + 1C + 1O → 3CO + 2C + 2O	3.24×10^{-22}	3.34×10^{-3}	1.83×10^{-16}	1.53
6CO	6CO → 5CO + 1C + 1O	3.96×10^{-10}	0.10	2.59×10^{-6}	0.26×10^{2}

Table 4
The free energy barriers of the forward (E_a) and reverse ($E_{a,r}$) reaction, and reaction rate (r_{dis}) at the temperature of 500 K for CO dissociation at different coverage over Co(0001) and Co(100) surfaces.

nCO	Dissociation route	E_a/kJ mol^{-1}	$E_{a,r}$/kJ mol^{-1}	r_{dis}/s^{-1} site^{-1}
Co(0001) surface				
1CO	1CO → 1C + 1O	235.0	140.5	-2.47×10^{-4}
2CO	2CO → 1CO + 1C + 1O	249.5	126.4	-8.0×10^{-3}
	1CO + 1C + 1O → 2C + 2O	260.4	99.5	−20.71
Co(100) surface				
1CO	1CO → 1C + 1O	131.0	177.0	0.02
2CO	2CO → 1CO + 1C + 1O	146.9	271.1	8.09×10^{-4}
	1CO + 1C + 1O → 2C + 2O	236.9	183.6	-3.39×10^{-7}
3CO	3CO → 2CO + 1C + 1O	140.3	164.5	4.44×10^{-3}
	2CO + 1C + 1O → 1CO + 2C + 2O	141.0	135.6	-1.16×10^{-3}
	1CO + 2C + 2O → 3C + 3O	213.2	197.2	-2.90×10^{-9}
4CO	4CO → 3CO + 1C + 1O	157.8	273.8	8.40×10^{-5}
	3CO + 1C + 1O → 2CO + 2C + 2O	241.0	250.8	9.91×10^{-14}
	2CO + 2C + 2O → 1CO + 3C + 3O	286.0	194.5	-5.50×10^{-8}
	1CO + 3C + 3O → 4C + 4O	246.3	10.1	-1.81×10^{11}
5CO	5CO → 4CO + 1C + 1O	142.4	243.8	3.41×10^{-3}
	4CO + 1C + 1O → 3CO + 2C + 2O	330.3	242.1	-2.61×10^{-14}
6CO	6CO → 5CO + 1C + 1O	214.6	227.6	1.26×10^{-12}

which is quite stable at a wide temperature. The third, fourth and fifth regions show the coverages of 4/9–5/9, 2/9–3/9 and 1/9 ML (n_{CO} = 4–5, 2–3 and 1), respectively, and they have comparatively narrow temperature ranges. The last region is the clean surface and free from CO molecules. From this phase diagram, we can obtain the equilibrium of coverage change at the corresponding temperature, for example, at standard atmospheric pressure, the first CO desorption starts from n_{CO} = 7 to 6 at 80 K (7/9–6/9 ML), the second CO desorption starts from n_{CO} = 6 to 5 at 510 K (6/9–5/9 ML), the third CO desorption starts from n_{CO} = 5 to 4 at 620 K (5/9 to 4/9 ML), the fourth CO desorption starts from n_{CO} = 3 to 2 at 700 K (3/9–2/9 ML), and the final CO desorption starts from 1/9 ML to become a clean surface at 700–810 K. Under ultra-high vacuum conditions, the full desorption of the adsorbed CO molecules takes places in the temperature range of 260–420 K. Kuipers et al. [56] have found that the behavior up to 490 K can be explained in terms of a decrease in CO coverage with the increasing of temperature. Wintterlin et al. [57] also shown that the dissociation of CO at CO pressures up to 0.25 mbar and the temperature up to 493 K by *in situ* scanning tunneling microscopy on Co(0001). Lahtinen et al. [14] have presented the $(\sqrt{7/3} \times \sqrt{7/3})$R 10.9°CO structure in a small coverage range around θ = 0.43 ML and the $(\sqrt{12/7} \times \sqrt{12/7})$R 10.9° structure with θ = 0.58 ML at saturation exposure at 180 K from the X-ray photoelectron spectroscopy, thermal desorption spectroscopy (TDS) and low energy electron diffraction. Both theory and experiment agree very reasonably.

On Co(100) surface (see Fig. 7), we also computed both the molecular and dissociative desorption states as well as the temperatures. At the standard atmospheric pressure, the first CO desorption starts from n_{CO} = 7 to 6 at 210 K (7/9–6/9 ML), the second CO desorption starts from n_{CO} = 6 to 5 at 690 K (6/9–5/9 ML), the third CO desorption starts from n_{CO} = 5 to 4 at 710 K (5/9–4/9 ML), the fourth CO desorption starts from n_{CO} = 3 to 2 at 840 K (3/9–2/9 ML), and the final CO desorption starts from 1/9 ML to become a clean surface at 840–865 K. Under the ultra-high vacuum conditions, the full desorption of the adsorbed CO molecules takes places in the temperature range of 280–500 K. However, there are no available UHV experimental studies of CO desorption on Co(100) surface. Thus, our calculated CO desorption states and temperatures might provide some references for further investigations using modern surface science techniques and analytical methods.

Most interestingly, the phase diagram also provides the information about CO adsorption and dissociation at the high temperature and high partial pressure on Co(0001) and Co(100) surfaces. Such information is directly associated with the initial

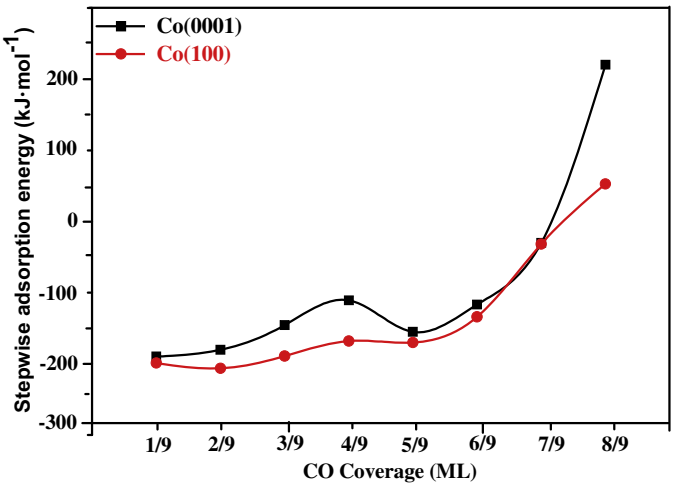

Fig. 8. The relationship between CO coverage and the stepwise adsorption free energy on Co(0001) and Co(100) surfaces at the temperature of 500 K.

stage of the Co-based FTS catalysts, where the surfaces are proved to be precovered with CO [9,58–59]. On the basis of these dates, it is interesting to investigate the effects of hydrogen in CO activation, either direct dissociation or hydrogen-assisted dissociation under the realistic reaction condition.

3.7. General discussion

The adsorption and the equilibrium between the dissociation and desorption of adsorbed CO molecules at different coverage have been clarified, in this section, the adsorption form of CO on two different Co surfaces will be identified, and the effect of coverage and surface morphology will be discussed.

For CO adsorption at different coverage over Co(0001) and Co(100) surfaces, with the increasing of coverage, the lateral repulsive interaction become stronger, and the stepwise adsorption free energy decreases (see Fig. 8), meanwhile, CO molecule start to move away from the initial site to balance the interaction. Hence, CO coverage has a few effects on both the adsorption site and strength of CO molecule on Co surface; moreover, the desorption free energies decreases with the increasing of CO coverage on both Co surfaces, which indicates that the higher CO coverage is, the easier CO desorption is. On the other hand, compared to Co(0001) surface, Co(100) has better activation ability for the C—O bond from the low coverage to the high coverage due to the high activity of 4 F hollow site.

The dissociation and desorption of these adsorbed CO molecules at different coverage are discussed to clarify the mechanism of CO initial activation process on the basis of the reaction free energy barrier and reaction rate constant, as well as the dissociation rate. For the adsorbed CO molecules over Co(0001) surface, it is found that the dissociation is unfavorable compared to the desorption from low to high coverage, suggesting that molecule adsorption CO is more preferred rather than its dissociation. While for the adsorbed CO molecules over Co(100) surface, as the coverage increases, the reaction free energy barrier of the first CO dissociation become higher, the corresponding rate constant become small, accordingly, the dissociation of CO become more and more difficult because of lower dissociation rate compared to the decreasing desorption energies. Therefore, the coverage affect CO dissociation on Co(100) surface, and Co(100) surface structure is more favorable for CO dissociation than the structure of Co(0001) surface; as a result, the adsorption form of CO is mainly determined by the surface structures.

4. Conclusions

In this study, the adsorption, dissociation and desorption of CO molecules at different coverage over Co surfaces have been systematically investigated with density functional theory calculations. It is found that the saturated adsorption on Co(0001) and (100) surfaces are 7/9 ML, meanwhile, on these two surfaces, the lateral repulsive interaction begins to affect the adsorption structures and the corresponding adsorption energies of these adsorbed CO molecules, and the interaction will became stronger with the increasing of CO coverage, which leads to CO migration over Co surfaces. Meanwhile, the adsorption free energies decrease gradually with the increasing of CO coverage until to the saturated adsorption. Moreover, the respective stretching frequencies of CO molecule at different coverage agree with the available experimental data. On the other hand, based on the stepwise adsorption configurations, only molecule adsorption CO is favored over (0001) surface; while on Co(100) surface, when the coverage is 1/9 ML, CO dissociation is easily than its desorption. When the coverage is from 2/9 to 5/9 ML, only the first CO dissociation is preferred, while desorption is more favored for the other CO molecules; when the coverage is greater than or equal to 6/9 ML, CO desorption will be more favorable than its dissociation. Generally speaking, we can come to a conclusion that the coverage of CO has effects on the adsorption site and strength, as well as the dissociation of CO molecule on Co surfaces, however, the surface structures affect the adsorption form of CO molecule in a large extent.

Acknowledgments

This work is financially supported by the National Natural Science Foundation of China (No. 21273265, 21203232, 21303241, 21503252, and 21276171). The authors are grateful to Dr. Xiaohu Yu who works at the Moscow Institute of Physics and Technology, for helpful discussion. The authors are grateful to Lvliang's cloud computing center for high-performance computing for CPU.

Appendix A. Supplementary data

Supplementary data associated with this article can be found, in the online version, at http://dx.doi.org/10.1016/j.apcata.2016.06.013.

References

[1] V. Subramani, S.K. Gangwal, Energy Fuels 22 (2008) 814–839.
[2] M. Gupta, M.L. Smith, J.J. Spivey, ACS Catal. 1 (2011) 641–656.
[3] M.A. Haider, M.R. Gogate, R.J. Davis, J. Catal. 261 (2009) 9–16.
[4] K.G. Fang, D.B. Li, M.G. Lin, M.L. Xiang, W. Wei, Y.H. Sun, Catal. Today 47 (2009) 133–138.
[5] J.J. Spivey, A. Egbebi, Chem. Soc. Rev. 36 (2007) 1514–1528.
[6] Y.Y. Liu, K. Murata, M. Inaba, I. Takahara, K. Okabe, Fuel 4 (2013) 62–69.
[7] E. Iglesia, Design. Appl. Catal. A: Gen. 161 (1997) 59–78.
[8] B.H. Davis, Ind. Eng. Chem. Res. 46 (2007) 8938–8945.
[9] M. Ojeda, R. Nabar, A.U. Nilekar, A. Ishikawa, M. Mavrikakis, E. Iglesia, J. Catal. 272 (2010) 287–297.
[10] J. Cheng, P. Hu, P. Ellis, S. French, G. Kelly, C.M. Lok, J. Phys. Chem. C 114 (2010) 1085–1093.
[11] C.F. Huo, Y.W. Li, J.G. Wang, H.J. Jiao, J. Phys. Chem. C 112 (2008) 14108–14116.
[12] S. Shetty, R.A. van Santen, Catal. Today 171 (2011) 168–173.
[13] M.E. Bridge, C.M. Comerie, R.M. Lambert, Surf. Sci. 67 (1977) 393–404.
[14] J. Lahtinen, J. Vaari, K. Kauraala, Surf. Sci. 418 (1998) 502–510.
[15] H. Papp, Surf. Sci. 129 (1983) 205–218.
[16] J. Lahtinen, J. Vaari, K. Kauraala, E.A. Soares, M.A. Van Hove, Surf. Sci. 448 (2000) 269–278.
[17] F. Greuter, D. Heskett, E.W. Plummer, H.J. Freund, Phys. Rev. B 27 (1983) 7117–7135.
[18] H. Papp, Surf. Sci. 149 (1985) 460–470.
[19] Q.F. Ge, M. Neurock, J. Phys. Chem. B 110 (2006) 15368–15380.
[20] J. Cheng, P. Hu, P. Ellis, S. French, G. Kelly, C.M. Lok, J. Phys. Chem. C 112 (2008) 9464–9473.
[21] Q. Gong, R. Raval, P. Hu, Surf. Sci. 562 (2004) 247–256.

[22] L. Joos, I.A.W. Filot, S. Cottenier, E.J.M. Hensen, M. Waroquier, V.V. Speybroeck, R.A. van Santen, J. Phys. Chem. C 118 (2014) 5317–5327.
[23] J.X. Liu, H.Y. Su, D.P. Sun, B.Y. Zhang, W.X. Li, J. Am. Chem. Soc. 135 (2013) 16284–16287.
[24] O. Kitakami, H. Sato, Y. Shimada, F. Sato, M. Tanaka, Phys. Rev. B 56 (1997) 13849–13854.
[25] N. Fischer, E. van Steen, M. Claeys, Catal. Today 171 (2011) 174–179.
[26] L. Braconnier, E. Landrivon, I. Cleímençon, C. Legens, F. Diehl, Y. Schuurman, Catal. Today 215 (2013) 18–23.
[27] G. Prieto, P. Concepcioín, R. Murciano, A. Martínez, J. Catal. 302 (2013) 37–48.
[28] P.E. Blöchl, Phys. Rev. B 50 (1994) 17953–17979.
[29] G. Kresse, D. Joubert, Phys. Rev. B 59 (1999) 1758–1775.
[30] G. Kresse, J. Furthmuller, Phys. Rev. B 54 (1996) 11169–21118.
[31] G. Kresse, J. Furthmuller, Comput. Mater. Sci. 6 (1996) 15–50.
[32] J.P. Perdew, J.A. Chevary, S.H. Vosko, K.A. Jackson, M.R. Pederson, D.J. Singh, C. Fiolhais, Phys. Rev. B 6 (1992) 6671–6687.
[33] S.G. Louie, S. Froyen, M.L. Cohen, Phys. Rev. B 26 (1982) 1738–1742.
[34] Q. Ge, M. Neurock, H.A. Wright, N. Srinivasan, J. Phys. Chem. B 106 (2002) 2826–2829.
[35] D.R. Lide, H.P.R. Frederikse, CRC Handbook of Chemistry and Physics, CRC Press, 1997.
[36] M. Zhuo, K.F. Tan, J. Phys. Chem. C 113 (2009) 8357–8365.
[37] N.W. Aschroft, N.D. Mermin, Solid State Physics, Holt, Rinehart, Winston, New York, 1976.
[38] J.C.W. Swart, E. van Steen, I.M. Ciobîcă, R.A. van Santen, Phys. Chem. Chem. Phys. 115 (2009) 803–807.
[39] B. Hao, Q. Wang, D.B. Li, R.G. Zhang, B.J. Wang, RSC Adv. 4 (2014) 43004–43011.
[40] Y.H. Zhao, M.M. Yang, D.P. Sun, H.Y. Su, K.J. Sun, X.F. Ma, X.H. Bao, W.X. Li, J. Phys. Chem. C 115 (2011) 18247–18256.
[41] J.A. Dean, Lange's Handbook of Chemistry, 15th edn., McGraw-Hill, 1999.
[42] D. Sheppard, P. Xiao, W. Chemelewski, D.D. Johnson, G. Henkelman, J. Chem. Phys. 136 (2012) 074103-1–074103-8.
[43] D. Sheppard, R. Terrell, G. Henkelman, J. Chem. Phys. 128 (2008) 134106-1–134106-10.
[44] G. Henkelman, H. Jónsson, J. Chem. Phys. 111 (1999) 7010–7022.
[45] R.A. Olsen, G.J. Kroes, G. Henkelman, A. Arnaldsson, H. Jónsson, J. Chem. Phys. 121 (2004) 9776–9792.
[46] A.Y. Khodakov, Catal. Today 144 (2009) 251–257.
[47] K. Reuter, M. Scheffler, Phys. Rev. B 65 (2001) 035406-1–035406-11.
[48] K. Reuter, M. Scheffler, Phys. Rev. B 68 (2003) 045407-1–045407-11.
[49] W.X. Li, C. Stampfl, M. Scheffler, Phys. Rev. B 68 (2003) 165412-1–165412-4.
[50] H. Yu, A.R. Oganov, I.A. Popov, G.R. Qian, A.I. Boldyrev, Angew. Chem. Int. Ed. 54 (2015) 1–6.
[51] H. Yu, X.M. Zhang, S.G. Wang, G.A. Feng, Appl. Surf. Sci. 343 (2015) 33–40.
[52] T. Wang, X.X. Tian, Y.W. Li, J.G. Wang, M. Beller, H.J. Jiao, J. Phys. Chem. C 118 (2014) 1095–1101.
[53] T. Wang, Y.W. Li, J.G. Wang, M. Beller, H.J. Jiao, J. Phys. Chem. 118 (2014) 3162–3171.
[54] J.K. Nørskov, F. Abild-Pedersen, F. Studt, T. Bligaard, Proc. Natl. Acad. Sci. U. S. A. 108 (2011) 937–943.
[55] H.A. Marzouk, E.B. Bradley, K.A. Arunkumar, Spectrosc. Lett. 18 (1985) 189–203.
[56] G.A. Beitel, A. Laskov, H. Oosterbeek, E.W. Kuipers, J. Phys. Chem. 100 (1996) 12494–12502.
[57] B. Böller, M. Ehrensperger, J. Wintterlin, ACS Catal. 5 (2015) 6802–6806.
[58] C.A. Mims, L.E. McCandlish, J. Phys. Chem. 91 (1987) 929–937.
[59] B.T. Loveless, C. Buda, M. Neurock, E. Iglesia, J. Am. Chem. Soc. 135 (2013) 6107–6121.